JACS
JOURNAL OF THE AMERICAN CHEMICAL SOCIETY

COMMUNICATION

pubs.acs.org/JACS

High-Speed *in situ* Surface X-ray Diffraction Studies of the Electrochemical Dissolution of Au(001)

Frederik Golks,[†,‡] Klaus Krug,[†,§] Yvonne Gründer,[†,#] Jörg Zegenhagen,[‡] Jochim Stettner,[†] and Olaf M. Magnussen*[,†]

[†]Institut für Experimentelle und Angewandte Physik, Universität Kiel, Leibnizstrasse 19, 24098 Kiel, Germany

[‡]European Synchrotron Radiation Facility, 6 Rue Jules Horowitz, 38000 Grenoble, France

ABSTRACT: We present *in situ* X-ray surface diffraction studies of interface processes with data acquisition rates in the millisecond regime, using the electrochemical dissolution of Au(001) in Cl-containing solution as an example. This progress in time resolution permits monitoring of atomic-scale growth and etching processes at solid−liquid interfaces at technologically relevant rates. Au etching was found to proceed via a layer-by-layer mechanism in the entire active dissolution regime up to rates of ∼20 ML/s. Furthermore, we demonstrate that information on the lateral surface morphology and in-plane lattice strain during the electrochemical process can be obtained.

High-resolution *in situ* studies of solid−liquid interfaces by structure-sensitive methods, such as scanning probe microscopy and synchrotron-based techniques, have become an indispensable tool in modern interface science. Specifically, they have contributed enormously to the in-depth understanding of the complex interface processes in crystal growth and dissolution by revealing in detail the mechanisms of nucleation and growth on the atomic scale. For example, in the field of electrochemical deposition or dissolution, these studies clarified the potential-dependent growth behavior and resulting nanoscale morphology in the early stages of deposition or dissolution. They revealed the influence of surface defects and heterogeneities on the initial nucleation in the submonolayer regime. Furthermore, they showed how the substrate as well as anionic or organic adsorbates affect the homogeneous nucleation densities and the shape of monolayer or vacancy islands, and allowed even the propagation of individual kinks to be followed along steps during growth or dissolution.[1,2]

Despite the unquestionable importance of these results for nanoscale electrochemistry, a common general problem of all of these studies is the low growth rates, which are at most a couple of monolayers (ML) per minute, but typically much lower. In contrast, the minimum current densities typically employed in technological electroplating, e.g., in the copper damascene process used in ULSI manufacturing,[3] are in the range of 10 $mA \cdot cm^{-2}$, corresponding to local growth rates of ≥10 ML/s. Hence, like in heterogeneous catalysis, where industrial processes and scientific model studies under ultra-high vacuum-conditions are separated by a huge "pressure gap", a substantial "current density gap" exists between atomic-resolution *in situ* studies and applications. Since the deposition rate (i.e., the flux of particles to the crystal surface) is a central parameter in kinetic growth theory and influences the growth behavior as well as the resulting deposit morphology,[4−6] this is a serious drawback in clarifying the mechanisms of real-world electrodeposition processes.

in situ studies at high growth rates by high-resolution scanning probe microscopy are difficult due to the inherently low image acquisition rates and the influence of the scanning tip. The former can be somewhat mitigated by progress in increasing the time resolution.[7] The latter is a fundamental problem, leading to significant shielding of the scanned area and consequently to orders of magnitude lower local growth rates.[8,9] In contrast, studies by photon-based methods, such as X-ray diffraction, are in principle not plagued by such interference by the experimental probe. However, before now most studies have been performed in thin-layer electrochemical cells, where the sample surface is covered by an electrolyte layer of only a few tens micrometers thickness. This results not only in a large ohmic drop but also in strongly hindered transport to the electrode surface. Thus, true *in situ* studies during electrochemical growth processes are not possible in this way.

As we recently demonstrated for the case of Au electrochemical deposition and dissolution in Cl-containing solution,[10−12] the growth behavior and interface structure can be directly followed by surface X-ray scattering (SXS) using synchrotron radiation. By employing a transmission geometry, electrochemical cells can be realized that — contrary to thin-layer SXS cells — feature unrestricted mass transport and time constants comparable to those achieved with conventional electrochemical cells. *in situ* measurements during growth or dissolution at moderate rates (a few seconds per ML) were possible with such cells, with the local microscopic rates being almost identical to the macroscopic rates derived from the current density. These studies revealed a layer-by-layer dissolution mechanism for the electrochemical dissolution of Au(111) up to the onset of passivation[12] and a complex, potential-dependent growth behavior, featuring step-flow, layer-by-layer, 3D, and re-entrant layer-by-layer growth, for the homoepitaxial electrodeposition of Au on Au(001).[10,11]

Here we demonstrate for the case of electrochemical dissolution of Au(001) that, even at rates approaching those employed in technological deposition and dissolution processes, atomic-scale data can be obtained by *in situ* surface X-ray diffraction. Key to this improvement was the implementation of a fast 1D X-ray detector (Dectris Mythen 1K). It permits a much higher data

Received: December 23, 2010
Published: February 22, 2011

dx.doi.org/10.1021/ja1115748 | *J. Am. Chem. Soc.* 2011, 133, 3772–3775

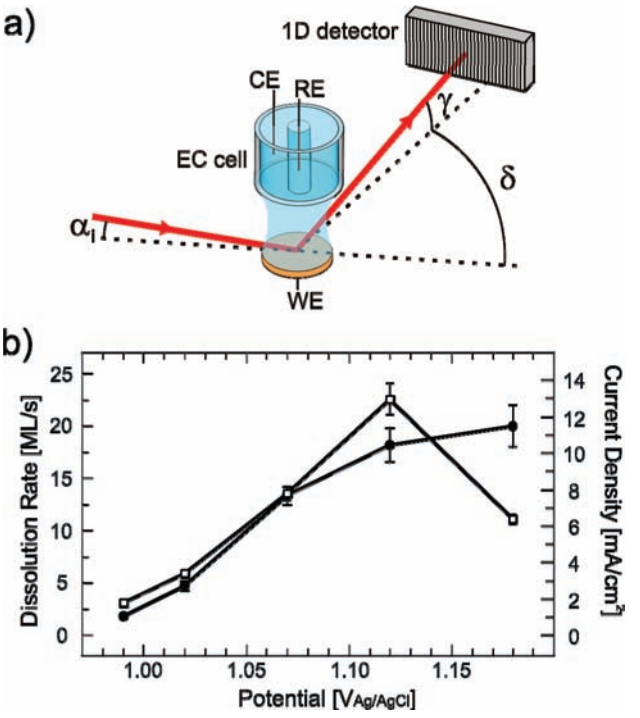

Figure 1. (a) Schematic scattering geometry of the *in situ* SXS experiments. (b) Potential-dependent microscopic dissolution rates obtained from the SXS experiments (filled circles) and from the simultaneously measured average electrochemical current density (open squares).

acquisition rate (up to 600 Hz) as compared to a conventional NaI point detector (maximum acquisition rate ~10 Hz). Furthermore, it allows simultaneously recording of the full diffraction peak cross section and the background scattering. As will be shown below, this enables measurements with millisecond data acquisition times, even at reciprocal space positions close to the surface-sensitive anti-Bragg position of the crystal truncation rod (CTR), where the intensity is minimal. This substantial progress in time resolution permits studies in a new time domain for single-shot surface diffraction experiments.

The measurements were performed using the six-circle diffractometer of beamline ID32 of the European Synchrotron Radiation Facility (ESRF) and the "hanging meniscus" X-ray transmission cell described in ref 13. The electrolyte is in contact with the sample electrode via a freestanding meniscus kept in an argon atmosphere (see scheme in Figure 1a). The incident X-ray beam (photon energy 22.5 keV), which is defined by vertical and horizontal slits of 10 and 300 μm, respectively, impinged at a grazing incident angle $\alpha_i = 0.384°$ onto the center of the electrode surface (corresponding to an illuminated sample area of 1.49×0.30 mm^2). Due to this wall-free geometry, the beam is only scattered by the sample and the electrolyte solution, and the background scattering is predominantly given by the smoothly varying liquid structure factor of the electrolyte solution. In order to minimize possible radiolytic effects, a fast photon shutter assured that the sample was only illuminated by the X-ray beam when recording the scattered intensity.

A NaI point detector was mounted together with the 1D detector on the same detector arm, which allows the former to be used for sample alignment and subsequently the latter for the time-resolved measurements. The 1D detector was oriented with the 1D pixel line parallel to the surface plane (see Figure 1a), covering an in-plane angular range of 3.66°. The spacing of the individual 50 μm wide pixels defined an angular resolution of $\Delta\delta = 2.865 \times 10^{-3}$°. Their height of 8 mm covered an angular range of $\Delta\gamma = 0.458°$ relative to the surface plane, over which the scattered intensity was integrated. In the time-resolved measurements, the Mythen detector was triggered by the potentiostat (Ivium, CompactStat), providing a precise temporal correlation of the X-ray time scan and the electrochemical data.

The samples used were 4 mm diameter Au(001) single crystals (Mateck) with a miscut <0.1° and a mosaic spread <0.013°, prepared by flame annealing prior to the experiment. The employed 0.1 M HCl + 0.5 mM $HAuCl_4$ electrolyte solution was prepared from HCl (Merck Ultrapur, 30%), $HAuCl_4$ aqueous solution (Chempur, 40% Au), and Milli-Q water. Potentials were measured versus a Ag/AgCl (3 M KCl) reference electrode. As coordinate system the common fcc Au unit cell with lattice constant $a = 4.08$ Å was employed.

The SXS studies were performed at the (1,1,0.1) position, i.e., close to the anti-Bragg position of the (1 1 l) crystal truncation rod. At this point in reciprocal space, the scattered intensity is highly sensitive to the surface morphology, specifically the atomic-scale roughness, and consequently provides insight into the growth or dissolution behavior in time-resolved measurements.[6,10−12] In the experiments, the sample was initially kept at 0.6 V, i.e., clearly below the Nernst potential of 0.83 V. The Au surface transport in this potential regime is fast, resulting in rapid smoothing of the surface.[10] SXS measurements at 0.6 V reveal a pronounced peak at (1,1,0.1) in the 1D detector frames with a height $>2 \times 10^4$ counts/s, allowing statistically significant single-shot measurements even at acquisition times of 5 ms (Figure 2a, inset).

The electrochemical Au dissolution was studied by stepping the potential to values in the range from 0.99 to 1.18 V, corresponding to overpotentials ≥160 mV and dissolution currents >1 mA·cm^{-2} (Figure 1b). As illustrated in Figure 2a, for a potential step to 1.07 V this resulted in dramatic changes in the initially constant integrated background-corrected intensity obtained from the 1D detector frames. In particular, regular oscillations in intensity are observed as a function of dissolution time, which are characteristic for a layer-by-layer dissolution mechanism. Similar oscillations were obtained up to dissolution potentials of 1.18 V but were most pronounced at the lowest overpotentials (see Figure 2b). Toward more positive potentials the SXS intensity rapidly decays with time (see Figure 2a), indicating an increasing surface roughening at higher dissolution rates, i.e., an imperfect layer-by-layer dissolution mechanism. A similar behavior was found in previous SXS studies of Au(111) performed at lower dissolution rates.[12] The microscopic dissolution rates, derived from the oscillation period, are in accordance with the simultaneously obtained electrochemical current densities (Figure 1b). The discrepancy at the most positive potentials is related to the onset of Au passivation in that range.

Atomic-scale data on Au(100) dissolution in chloride-containing electrolyte were also obtained in an earlier *in situ* STM study by Ye et al.,[14] albeit at much lower dissolution rates (<0.1 ML/min). In this work dissolution occurred predominantly by step flow etching, with the steps in the dissolution regime exhibiting a strong preferential orientation along the [100] directions of the Au substrate. Our results indicate a transition toward layer-by-layer or smooth multilayer (see ref 12) dissolution at higher overpotentials, illustrating the importance of *in situ* studies at realistic current densities.

dx.doi.org/10.1021/ja1115748 |*J. Am. Chem. Soc.* 2011, 133, 3772–3775

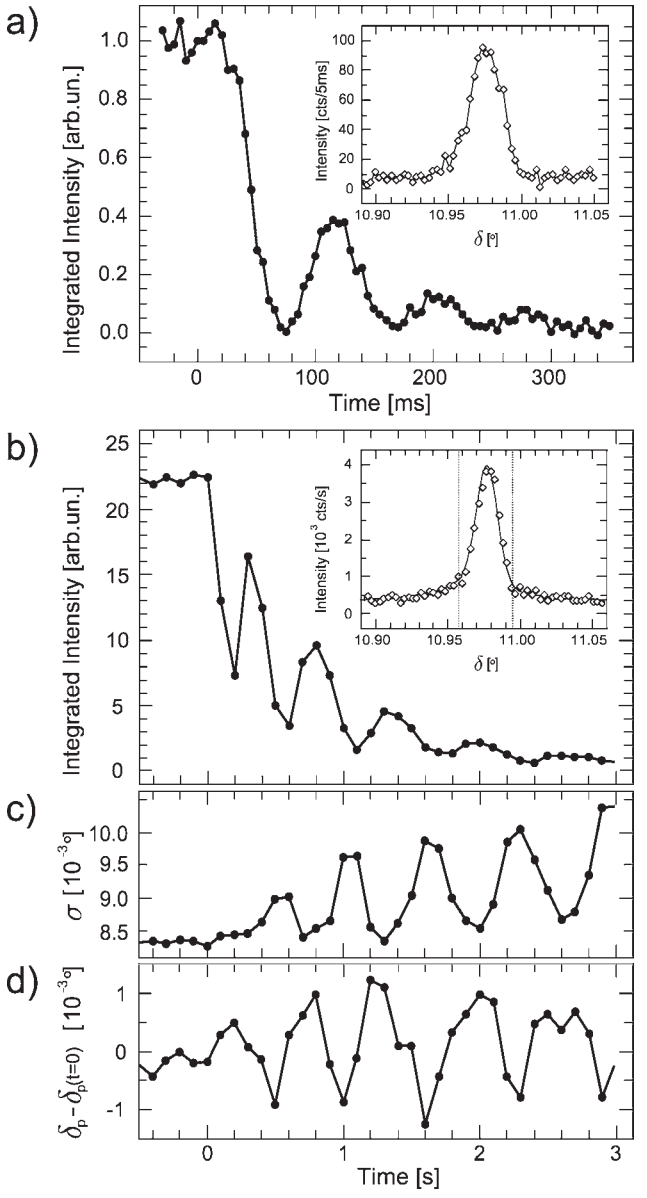

Figure 2. *in situ* SXS intensity of Au(001) in 0.1 M HCl + 0.5 mM $HAuCl_4$ at (1,1,0.1) during potential steps from 0.6 to (a) 1.07 (200 frames/s) and (b−d) 0.99 V (10 frames/s), showing growth oscillations in the Au dissolution regime (filled circles). Insets show selected single frames of the 1D detector obtained at (a) t = 15 ms and (b) t = 1.9 s (the dashed line indicates the limited range used for the determination of σ and δ_p). In addition, for the step to 0.99 V, (c) the peak width σ and (d) the peak position δ_p of the (1,1,0.1) peak are shown.

Each frame of the 1D detector provides not only the integrated peak intensity but also additional structural information with the same temporal resolution. This is illustrated by results of a dissolution experiment at 0.99 V (recorded with 100 ms/frame to improve the counting statistics), where in addition to the peak intensity the peak position δ_p and peak width σ were determined as a function of dissolution time (Figure 2b−d). Due to a slight asymmetry in the peak shape (see below), the latter two values were determined by calculating the first and second moment (mean value and its standard deviation, respectively) of the δ-dependent intensity distribution (limited to the range indicated by the dashed lines in the inset in Figure 2b to reduce the effect of the broad background peak). Fits of the peak by a Gaussian resulted in peak positions and heights with a qualitatively very similar behavior; i.e., the results discussed below are robust with respect to the analysis method.

As clearly visible, not only the intensity but also the width of the CTR peak oscillate in the dissolution regime (Figure 2c), with maxima and minima in intensity corresponding to particularly narrow and broad peaks, respectively. The oscillating peak width indicates the changes in the size of the coherently scattering regions on the sample surface and agrees well with expectations for layer-by-layer growth: at maxima in intensity, the topmost layer is approximately closed (coverage close to 1) and the X-ray correlation length is determined (apart from the instrumental resolution) by the average size of the terraces between atomic steps in the substrate. In contrast, the minima in intensity correspond to a surface covered by approximately half a monolayer of Au etch pits ("vacancy islands"), and the correlation length is given by the average size of the pits and the (comparably sized) areas between them. The correlation length hence is significantly smaller than the terrace size, resulting in a larger peak width.

Also the peak position δ_p oscillates in-phase with the peak intensity, indicating oscillations in the lattice spacing (Figure 2d). This behavior can be rationalized by an in-plane lattice expansion in the topmost Au layer at partial coverage. Under these conditions, the finite extension of the remaining Au islands between the etch pits allows lateral relaxation. From the minima in δ_p, a strain of the order of 10^{-4} is calculated for the experiment in Figure 2b. Similar observations with even larger lattice expansions were reported for vapor-phase Cu(001) homoepitaxial growth.[15] A more detailed analysis suggests the presence of two overlapping peaks at slightly different positions, resulting in an asymmetric peak shape. A similar behavior was reported previously in SXS studies of vapor-phase epitaxial growth.[16] The peak asymmetry also oscillates in-phase with the intensity oscillations (manifested in oscillations in the third moment of the intensity distribution), indicating different responses of the two peaks to the morphological changes during dissolution. A more detailed quantitative analysis of such effects will be presented elsewhere.

These preliminary studies illustrate the potential of *in situ* SXS for gaining detailed structural information on the growth interface during realistic deposition conditions. In fact, a clear diffraction peak at (1,1,0.1) was even observable at an acquisition rate of 500 Hz, which means that *in situ* measurements at deposition or dissolution rates up to 100 ML/s are, in principle, feasible. Systematic studies of this type will provide fundamental insight into technologically relevant electrochemical processes. Furthermore, they will allow experimental testing of the applicability of modern growth theories to electrochemical deposition and dissolution processes.

AUTHOR INFORMATION

Corresponding Author
magnussen@physik.uni-kiel.de

Present Addresses
[§]Department of Chemical Engineering, National Cheng Kung University, Tainan 70101, Taiwan.
[#]The School of Chemistry, The University of Manchester, Oxford Road, Manchester M13 9PL, UK.

■ ACKNOWLEDGMENT

We thank the DFG for financial support via MA1618/13-3 and the staff of ID 32 for technical assistance. We acknowledge the European Synchrotron Radiation Facility for provision of synchrotron radiation facilities.

■ REFERENCES

(1) Itaya, K. *Prog. Surf. Sci.* **1998**, *58*, 121.
(2) Magnussen, O. M.; Behm, R. J. *J. Electroanal. Chem.* **1999**, *467*, 258.
(3) Andricacos, P. C.; Uzoh, C.; Dukovic, J. O.; Horkans, J.; Deligianni, H. *IBM J. Res. Develop.* **1998**, *42*, 567.
(4) Venables, J. A.; Spiller, G. D. T.; Hanbrücken, M. *Rep. Prog. Phys.* **1984**, *47*, 399.
(5) Brune, H. *Surf. Sci. Reports* **1998**, *31*, 121.
(6) Rosenfeld, G.; Poelsema, B.; Comsa, G. In *Growth and properties of ultrathin epitaxial layers*; King, D. A., Woodruff, D. P., Eds.; Elsevier Science B.V.: Amsterdam, 1999; Vol. 8, p 66.
(7) Polewska, W.; Behm, R. J.; Magnussen, O. M. *Electrochim. Acta* **2003**, *48*, 2915.
(8) Divisek, J.; Steffen, B.; Stimming, U.; Schmickler, W. *J. Electroanal. Chem.* **1997**, *440*, 169.
(9) Skylar, O.; Treutler, T. H.; Vlachopoulos, N.; Wittstock, G. *Surf. Sci.* **2005**, *597*, 181.
(10) Krug, K.; Stettner, J.; Magnussen, O. M. *Phys. Rev. Lett.* **2006**, *96*, 246101–1.
(11) Kaminski, D.; Krug, K.; Golks, F.; Stettner, J.; Magnussen, O. M. *J. Phys. Chem. C* **2007**, *111*, 17067.
(12) Krug, K.; Kaminski, D.; Golks, F.; Stettner, J.; Magnussen, O. M. *J. Phys. Chem. C* **2010**, *114*, 18634.
(13) Magnussen, O. M.; Krug, K.; Ayyad, A. H.; Stettner, J. *Electrochim. Acta* **2008**, *53*, 3449.
(14) Ye, S.; Ishibashi, C.; Uosaki, K. *Proc. Electrochem. Soc.* **2000**, *PV2000-35*, 133.
(15) Fassbender, J.; May, U.; Schirmer, B.; Jungblut, R. M.; Hillebrands, B.; Güntherodt, G. *Phys. Rev. Lett.* **1995**, *75*, 4476.
(16) Braun, W.; Kaganer, V. M.; Jenichen, B.; Satapathy, D. K.; Guo, X.; Tinkham, B. P.; Ploog, K. H. *J. Cryst. Growth* **2005**, *278*, 449–457.